Zeeman effect of the energy levels of Fe^{2+} in diluted magnetic semiconductors

Murielle Villeret and Sergio Rodriguez
Department of Physics, Purdue University, West Lafayette, Indiana 47907

E. Kartheuser
Institut de Physique, Université de Liège, B-4000 Liège 1, Belgium
(Received 21 February 1992)

We present a study of the magnetic-field dependence of the energy levels of Fe^{2+} in a wurtzite diluted magnetic semiconductor. We limit our considerations to transitions in the infrared region of the electromagnetic spectrum. The Hamiltonian of the ion has been diagonalized to fourth power in the parameter $|\lambda|/\Delta$, the ratio of the strength of the spin-orbit interaction λ to the splitting Δ arising from the tetrahedral component of the crystal potential. We make no *a priori* assumption concerning the relative strengths of λ and the parameters describing the effect on the crystal field of the trigonal distortion. The parameters describing the Fe^{2+} ion in CdSe are obtained from near-infrared absorption data at zero magnetic field by Udo *et al.* [Phys. Rev. B **46**, 7459 (1992)]. With these values we make a comparison with the electronic Raman-effect data obtained by Mauger *et al.* [Phys. Rev. B **43**, 7102 (1991)] as functions of the intensity and direction of an applied magnetic field.

I. INTRODUCTION

Following the intense investigation of the Mn-based diluted magnetic semiconductors[1] (DMS), i.e., compounds of the form $A_{1-x}Mn_xB$ where A and B are elements of the groups II and VI of the periodic chart, respectively, recent interest has concentrated on materials containing other transition-metal ions. In this paper we are concerned with the energy levels of Fe^{2+} occupying a cation site in a II-VI wurtzite semiconductor. In particular we focus our attention on the properties of $Cd_{1-x}Fe_xSe$.

We have previously reported a study of Fe^{2+} and Co^{2+} in both zinc-blende and wurtzite crystals[2] using perturbation theory. However, in view of the recent experimental results of Udo *et al.*,[3] it became obvious that the results of Ref. 2 should be extended to include higher-order terms in perturbation theory and a treatment of the spin-orbit interaction and the trigonal distortion on an equal footing. The results of Ref. 3 were concerned with the absorption in the near infrared in zero magnetic field of Fe^{2+} in both CdTe and CdSe. A number of transitions were identified which will be described briefly in Sec. V and are discussed in detail in Ref. 3. Studies of the electronic Raman spectrum of $Cd_{1-x}Fe_xSe$ as a function of magnetic field were carried out by Mauger *et al.*[4] Reference 4 is concerned exclusively with the Raman transitions between the ground state of Fe^{2+} and the next two electronic excitations which occur in the far infrared. The energy-level structure obtained in Ref. 3 also allows one to determine the position of the Raman lines in zero magnetic field.

In Sec. II we derive the 25×25 Hamiltonian matrix of the ground term ^5D of Fe^{2+} in a crystal potential in the presence of an external magnetic field. The 25 wave functions that we use are obtained from symmetry considerations using group-theoretical techniques. The diagonalization of the Hamiltonian in the framework of perturbation theory forms the scope of Sec. III. No *a priori* assumption is made regarding the relative strengths of the spin-orbit interaction and the trigonal distortion, which are treated on an equal footing.

Section IV is concerned with corrections arising from the mixing by the spin-orbit interaction of states originating from the orbital ground multiplet with excited levels. Finally, in Sec. V, we give some applications of the theory developed in the preceding sections. In particular, we show how perturbation theory can provide invaluable information about the phenomenological parameters λ and the crystal-field constants. We develop an iteration technique which, combined with the experimental results of Udo *et al.*,[3] allows us to get a first estimate of the parameters characterizing Fe^{2+} in CdSe. These are, later on, refined by numerical diagonalization of the Hamiltonian matrix. We then use these values to present a comparison with the Raman spectra of Mauger *et al.*[4]

II. HAMILTONIAN MATRIX FOR Fe^{2+} IN A WURTZITE CRYSTAL IN THE PRESENCE OF AN EXTERNAL MAGNETIC FIELD

The total Hamiltonian for a particular term (defined by L and S) of an ion in a crystal potential V_c, and in the presence of an external magnetic field of induction $\mathbf{B}$ is

$$H = H_0 + V_c + \lambda \mathbf{L}\cdot\mathbf{S} + \mu_B \mathbf{B}\cdot(\mathbf{L}+2\mathbf{S}) , \tag{1}$$

where H_0 is the Hamiltonian of the free ion excluding the spin-orbit interaction, $\lambda\mathbf{L}\cdot\mathbf{S}$, and in the Zeeman interaction we approximate the electron g factor, taking it to be equal to 2. The terms in the Hamiltonian (1) have been written in order of decreasing magnitudes.

We suppose that the most important part of V_c is tetrahedral with principal axes $\hat{x},\hat{y},\hat{z}$ and that in wurtzite there is a small distortion along [111] which we call the trigonal axis $\hat{\zeta}$. The site symmetry of the magnetic ion is

then C_{3v}. In a system of coordinates $\hat{\xi},\hat{\eta},\hat{\zeta}$ with $\hat{\xi}\|[11\bar{2}]$, $\hat{\eta}\|[\bar{1}10]$, and $\hat{\zeta}\|[111]$, the crystal potential takes the following form:[2,5]

$$V_c = V_c(T_d) + V_c(C_{3v}) , \tag{2}$$

where

$$V_c(T_d) = a' \sum_i \left[-\tfrac{1}{30}(35\zeta_i^4 - 30\zeta_i^2 r_i^2 + 3r_i^4) - \frac{2\sqrt{2}}{3}\zeta_i\xi_i(\xi_i^2 - 3\eta_i^2) \right] \tag{3}$$

and

$$V_c(C_{3v}) = \tfrac{1}{3}b' \sum_i (\xi_i^2 + \eta_i^2 - 2\zeta_i^2) + \frac{c'}{60}\sum_i (35\zeta_i^4 - 30\zeta_i^2 r_i^2 + 3r_i^4) . \tag{4}$$

The summation over i extends over all the electrons in the $3d$ shell. The trigonal distortion $V_c(C_{3v})$ is small compared to $V_c(T_d)$. However, it is necessary to include the effect of $V_c(C_{3v})$ in the description of the energy levels of the magnetic ion. The question that arises then concerns the order of magnitude of $V_c(C_{3v})$ compared to that of the other terms intervening in the Hamiltonian (1). This question and its consequences will be discussed in detail in Secs. III–V. For the time being we make no assumption regarding the relative orders of magnitude of the crystal potential, the spin-orbit interaction, and the Zeeman interaction, and derive the expression of the Hamiltonian matrix in the ^5D ground manifold of Fe^{2+}. To evaluate the matrix elements of the crystalline potential we use, as in our earlier work,[2,6–9] the method of operator equivalents introduced by Stevens.[10] In this formalism one replaces ξ,η,ζ by appropriate combinations of the components of the angular-momentum operator in such a way that the new expressions transform exactly as the original ones under the operations of the symmetry group of the site. This yields

$$V_c(T_d) = a(\tfrac{7}{6}L_\zeta^4 - \tfrac{31}{6}L_\zeta^2 + \tfrac{12}{5}) + \frac{a\sqrt{2}}{6}\{L_+^3 + L_-^3, L_\zeta\} \tag{5}$$

and

$$V_c(C_{3v}) = -b(2 - L_\zeta^2) - c(\tfrac{7}{12}L_\zeta^4 - \tfrac{31}{12}L_\zeta^2 + \tfrac{6}{5}) , \tag{6}$$

where $\{u,v\} = uv + vu$ and a, b, and c are phenomenological parameters[11] to be obtained from experiment (see Sec. V).

For the orbital states we choose the wave functions which diagonalize $V_c(T_d)$. (See Table VI of Ref. 2, with $\cos\alpha = 3^{-1/2}$.) They are

$$\begin{aligned} u_1 &= (\tfrac{2}{3})^{1/2}\phi_1 + 3^{-1/2}\phi_{-2} , \\ u_{-1} &= (\tfrac{2}{3})^{1/2}\phi_{-1} - 3^{-1/2}\phi_2 , \\ v_0 &= \phi_0 , \\ v_1 &= 3^{-1/2}\phi_1 - (\tfrac{2}{3})^{1/2}\phi_{-2} , \\ v_{-1} &= 3^{-1/2}\phi_{-1} + (\tfrac{2}{3})^{1/2}\phi_2 , \end{aligned} \tag{7}$$

where ϕ_μ ($\mu = 2,1,0,-1,-2$) are the eigenstates of the projection of the orbital angular-momentum operator $\mathbf{L}$ along the $\hat{\zeta}$ axis. v_0 belongs[12] to $\Gamma_1(C_{3v})$, whereas the pairs (u_1,u_{-1}) and (v_1,v_{-1}) belong to $\Gamma_3(C_{3v})$; the subindices 1 and -1 indicate that they behave as $\phi_1 \sim -(\xi + i\eta)$ and $\phi_{-1} \sim \xi - i\eta$, respectively, under the operations of the group. Before proceeding further we evaluate the matrix elements of V_c in the states given in Eqs. (7). We obtain[13]

$$\begin{aligned} \langle u_1|V_c|u_1\rangle &= \langle u_{-1}|V_c|u_{-1}\rangle = -\tfrac{18}{5}a + \frac{7c}{15} , \\ \langle v_0|V_c|v_0\rangle &= \tfrac{12}{5}a - 2b - \tfrac{6}{5}c , \\ \langle v_1|V_c|v_1\rangle &= \langle v_{-1}|V_c|v_{-1}\rangle = \tfrac{12}{5}a + b + \frac{2c}{15} , \end{aligned} \tag{8}$$

and

$$\begin{aligned} \langle u_1|V_c|v_1\rangle &= \langle u_{-1}|V_c|v_{-1}\rangle \\ &= \langle v_1|V_c|u_1\rangle = \langle v_{-1}|V_c|u_{-1}\rangle \\ &= -2^{1/2}\left[b - \frac{c}{3}\right] . \end{aligned}$$

In order to include the effect of the spin-orbit coupling and the Zeeman interaction in the ^5D manifold, we start from a basis of 25 wave functions which are appropriate combinations of orbital and spin states. Let $\chi_\mu(\mu = 2,1,0,-1,-2)$ be the spin states. They are classified under the operations of C_{3v} as follows:

$$\begin{aligned} &\chi_0 \in \Gamma_1 , \\ &\chi_1, \chi_{-1} \in \Gamma_3 , \\ &\chi_{-2}, -\chi_2 \in \Gamma_3 . \end{aligned}$$

The choice of the second Γ_3 pair and the order of the functions are mandated by the need to have two sets of functions generating $\Gamma_3(C_{3v})$ in *identical* unitary form. The total wave functions are combinations of u_i, v_j, and χ_μ ($i = 1,-1; j = 1,0,-1; \mu = 2,1,0,-1,-2$), which can be obtained using the Clebsch-Gordan coefficients for C_{3v}. They are given in Appendix A together with their symmetry classification.

In the absence of an external magnetic field, the 25×25 Hamiltonian matrix splits into a 5×5, a 4×4, and two identical 8×8 submatrices, corresponding to the Γ_1, Γ_2, and Γ_3 states, respectively. The Zeeman interaction mixes Γ_1 with Γ_2 when $\mathbf{B}$ is along the trigonal axis $\hat{\zeta}$, and Γ_1 with Γ_3 when $\mathbf{B}\perp\hat{\zeta}$, contrary to the statement in Ref. 4. The Hamiltonian matrix in the presence of an external magnetic field can be decomposed into blocks of the form $M_{\mu\nu}$ ($\mu,\nu = \alpha,\beta,\gamma^{(+)},\gamma^{(-)}$) corresponding to the wave functions $\alpha_i,\beta_j,\gamma_k^{(+)},\gamma_k^{(-)}$ ($i = 1,2,\ldots,5; j = 1,2,\ldots,4; k = 1,2,\ldots,8$) given in Appendix A. The submatrices are given in Appendix B. We note that the 25×25 Hamiltonian matrix is Hermitian and that the diagonal blocks have dimensions 5, 4, and 8, respectively. The off-diagonal submatrices are rectangular matrices whose dimensions are obvious from their description in Appendix B. Calculation of these matrices is simplified by the use

of the time-reversal operator T. We note that

$$T\alpha_i=\alpha_i;\quad T\beta_j=\beta_j;\quad T\gamma_k^{(\pm)}=-\gamma_k^{(\mp)}$$

$(i=1,\ldots,5;j=1,\ldots,4;k=1,\ldots,8)$ so that

$$\langle\gamma_j^{(+)}|L_\xi|\gamma_i^{(+)}\rangle=-\langle\gamma_j^{(-)}|L_\xi|\gamma_i^{(-)}\rangle^*\ ,$$

$$\langle\gamma_j^{(+)}|L_+|\beta_i\rangle=\langle\gamma_j^{(-)}|L_-|\beta_i\rangle^*\ ,$$

and

$$\langle\gamma_j^{(+)}|L_+|\gamma_i^{(-)}\rangle=-\langle\gamma_j^{(-)}|L_-|\gamma_i^{(+)}\rangle^*\ .$$

Here $L_\pm=L_\xi\pm iL_\eta$.

III. PERTURBATION THEORY

The 25×25 Hamiltonian matrix derived in Sec. II can, of course, be diagonalized numerically. Such a diagonalization has indeed been performed and we will discuss its result in Sec. V. However, a numerical diagonalization does not give a physical understanding of the experimentally observed phenomena, e.g., optical absorption, magnetization, or Raman-scattering measurements, and reduces the determination of the phenomenological parameters λ, $\Delta=6a$, b, and c to a matter of sheer guessing. We will show that perturbation theory, on the other hand, provides useful physical insight, invaluable information about the parameters, and can even, when used with sufficient care and in the appropriate situation, give an accurate description of the experimental results. Even in those cases when it is not sufficiently accurate, it encompasses all the experimental features.

The starting point of the perturbation formalism is based on information on the relative strengths of the various terms intervening in the Hamiltonian (1). Of particular interest are the relative orders of magnitude of the spin-orbit interaction and the trigonal distortion. They are not known *a priori* but assumptions can be made regarding their strengths. The results obtained under these assumptions can be compared to the experiments and the phenomenological parameters extracted on a self-consistent basis. Such "feedback" provides information on the validity of the initial assumptions and, in turn, on the strength of the trigonal distortion. The results obtained from perturbation theory can then be refined by the numerical diagonalization.

In a previous work,[2] we had assumed that the trigonal crystal field was much smaller than the spin-orbit interaction, so that $V_c(C_{3v})$ could be treated as a perturbation on the spin-orbit-split states. The resulting corrections to the energies of the 25 lowest levels of Fe^{2+} obtained in this framework are given in Tables VII and VIII of Ref. 2. The validity, limitations, and usefulness of this type of perturbative formalism are discussed in Sec. V, taking the case of Fe^{2+} in CdSe as an example. From this first approach it can be inferred that greater accuracy would be obtained for the energies of the levels originating from the lowest orbital multiplet if the spin-orbit interaction and the trigonal field were treated on the same footing. The Zeeman interaction is still assumed to be small, a good approximation for magnetic fields below 60 kG since for this field $\mu_B B\lesssim3\ \mathrm{cm}^{-1}$.

We calculate the energies of the ten lowest levels of Fe^{2+} as a function of B for two orientations of the magnetic field with respect to the trigonal axis. $V_c(T_d)$ splits the orbital term into a doublet Γ_3 and a triplet Γ_5, each having a fivefold spin degeneracy. We neglect, for the time being, corrections due to mixing with the levels originating from the $^5\Gamma_5$ multiplet. These form the scope of Sec. IV.

When $\mathbf{B}\|\hat{\xi}$, in the $^5\Gamma_3$ manifold of Fe^{2+}, the Zeeman interaction mixes the states α_1, α_3, β_1, and β_3. The second-order perturbation matrix is

$$\mathcal{H}^{(2)}=-\frac{6\lambda^2}{\Delta}(2+\tfrac{1}{3}x+\tfrac{1}{3}x^2-M)\ , \tag{9}$$

where

$$M=\begin{bmatrix}-1+x & -2^{1/2} & i\nu & 0\\ -2^{1/2} & -x & 0 & -2i\nu\\ -i\nu & 0 & 1+x & 2^{1/2}\\ 0 & 2i\nu & 2^{1/2} & -x\end{bmatrix}\ . \tag{10}$$

Here $x=(3b-c)/3|\lambda|\equiv\kappa/|\lambda|$ is essentially the ratio of the trigonal field splitting and the spin-orbit splitting, whereas $\nu=(\mu_B B\Delta/3\lambda^2)$ is the ratio of the Zeeman interaction to the spin-orbit splitting. In the absence of an external magnetic field B the energies can be calculated exactly and the effect of B is obtained solving by iteration the secular equation corresponding to the Hamiltonian in Eqs. (9) and (10). The energies of the two Γ_1 and two Γ_2 states originating from $^5\Gamma_3$ are then of the form

$$E_i=-\frac{6\lambda^2}{\Delta}(2+\tfrac{1}{3}x+\tfrac{1}{3}x^2-p_i')\ , \tag{11}$$

with

$$p_i'=p_i+\nu^2(5p_i^2-6p_ix+5x^2+4)\prod_{j\neq i}(p_i-p_j)^{-1}$$

$$(i,j=1,\ldots,4)\ . \tag{12}$$

The p_i's are the eigenvalues of (10) in the absence of a magnetic field ($\nu=0$) and are given by

$$p_{1,2}(x)=-\tfrac{1}{2}\mp\tfrac{1}{2}[9-4x+4x^2]^{1/2} \tag{13}$$

corresponding to the two Γ_1 states and

$$p_{4,3}(x)=-p_{1,2}(-x) \tag{14}$$

corresponding to the Γ_2 states.

A magnetic field parallel to the trigonal axis also mixes the Γ_3 levels among themselves. The $\gamma_1^{(\pm)},\gamma_3^{(\pm)},\gamma_7^{(\pm)}$ perturbation matrices are

$$\mathcal{H}^{(\pm)}=-\frac{6\lambda^2}{\Delta}[2+\tfrac{1}{3}x^2-N_\pm]\ , \tag{15}$$

where

$$N_\pm=\begin{bmatrix}\mp\nu-2x/3 & 0 & 3^{-1/2}\\ 0 & \pm2\nu+4x/3 & -(\frac{2}{3})^{1/2}\\ 3^{-1/2} & -(\frac{2}{3})^{1/2} & 0\end{bmatrix}\ , \tag{16}$$

TABLE I. Energies of lines I, IIa, IIb and model parameters in cm^{-1}.

Experiment		Theory Perturbation	Theory Exact	Mauger *et al.* (Ref. 4)
		$\lambda=-93.3$	$\lambda=-94.0$	$\lambda=-95.3$
		$\Delta=2546.1$	$\Delta=2550.6$	$\Delta=2620$
		$b=12.5$	$b=28.0$	$b=17.5$
		$c=-28.1$	$c=-22.0$	$c=-39.3$
E_{I}	2375.4	2375.4	2375.4	2453.1
E_{IIa}	2362.8	2362.8	2362.8	2440.2
E_{IIb}	2358.0	2358.0	2358.0	2435.6

which can easily be diagonalized. The energies of the three lowest Γ_3 states are then of the form

$$E_i=-\frac{6\lambda^2}{\Delta}(2+\tfrac{1}{3}x^2-p_i) \quad (i=5,\ldots,10)\ , \tag{17}$$

where

$$p_{5,6}(\nu)=\tfrac{1}{3}x+\frac{\nu}{2}\mp[1+(x+3\nu/2)^2]^{1/2}\ , \tag{18}$$

$$p_{8,9}(\nu)=p_{5,6}(-\nu)\ , \tag{19}$$

and

$$p_{7,10}=0\ . \tag{20}$$

When the magnetic field is perpendicular to the trigonal axis all ten lowest levels are mixed. The energies at $B=0$ are, of course, known from what precedes and the effect of the magnetic field can be included as a perturbation.

IV. CORRECTIONS DUE TO MIXING OF THE $^5\Gamma_3$ AND $^5\Gamma_5$ ORBITAL STATES BY THE SPIN-ORBIT INTERACTION

The spin-orbit interaction $\lambda\mathbf{L}\cdot\mathbf{S}$ mixes the states associated with the $^5\Gamma_3$ and $^5\Gamma_5$ orbital multiplets, giving rise to corrections proportional to powers of the parameter $\sigma=|\lambda|/\Delta$. These corrections were taken into account, for example, in our study[9] of the magnetic properties of Fe^{2+} in cubic zinc-blende crystals, and are shown to be of importance by optical-absorption studies.[3,14] They have thus to be included in our study of Sec. III. For this purpose we first diagonalize the matrices in Eqs. (10) and (16) when $x=\nu=0$, then apply the corresponding unitary transformation to the complete matrices and include the corrections in σ on the diagonal using, for example, Table III of Ref. 9. When the magnetic field is along $\hat{\zeta}$, the energies of the Γ_1 and Γ_2 levels are still given by Eqs. (11) and (12) but now

$$p_{1,2}(x)=-\tfrac{1}{2}(1-7\sigma-79\sigma^2)\mp\tfrac{1}{2}[9(1-3\sigma-27\sigma^2)^2-4x(1-3\sigma-27\sigma^2)+4x^2]^{1/2} \tag{21}$$

and

$$p_{3,4}(x)=\tfrac{1}{2}(1+3\sigma+45\sigma^2)\mp\tfrac{1}{2}[9(1-\sigma-15\sigma^2)^2+4x(1-\sigma-15\sigma^2)+4x^2]^{1/2}\ . \tag{22}$$

A similar procedure can be followed to include the corrections proportional to σ in the energies of the Γ_3 states. The lowest Γ_3 level splits in a magnetic field into states with energies

$$E_{5,8}=-\frac{6\lambda^2}{\Delta}(2+\tfrac{1}{3}x^2-p'_{5,8})\ , \tag{23}$$

where

$$p'_{5,8}=p_{5,8}+\rho_1\sigma+\rho_2\sigma^2+\cdots\ , \tag{24}$$

p_5 and p_8 are given in Eqs. (18) and (19), and the expressions of the coefficients ρ_1 and ρ_2 are shown in Appendix C.

V. APPLICATIONS

The theory developed in Secs. II–IV provides the framework for the interpretation of experimental observations such as optical absorption,[3] Raman scattering,[4] or magnetic-susceptibility[15] studies. The constants λ, Δ, b, and c are taken as phenomenological parameters to be determined from the experiment. We show in this section how perturbation theory can be used to provide a first estimate of the parameters which, in turn, can be refined through numerical work. We take the case of

TABLE II. Matrix $M_{\alpha\alpha}$ of the Hamiltonian in the states α_i $(i=1,\ldots,5)$.

$M_{\alpha\alpha}$	α_1	α_2	α_3	α_4	α_5
α_1	0	$-\sqrt{2}(\kappa+\lambda)$	0	2λ	$2\sqrt{3}\lambda$
α_2	$-\sqrt{2}(\kappa+\lambda)$	$\Delta_1+\lambda$	-2λ	0	$\sqrt{6}\lambda$
α_3	0	-2λ	0	$\sqrt{2}(-\kappa+2\lambda)$	0
α_4	2λ	0	$\sqrt{2}(-\kappa+2\lambda)$	$\Delta_1-2\lambda$	0
α_5	$2\sqrt{3}\lambda$	$\sqrt{6}\lambda$	0	0	Δ_2

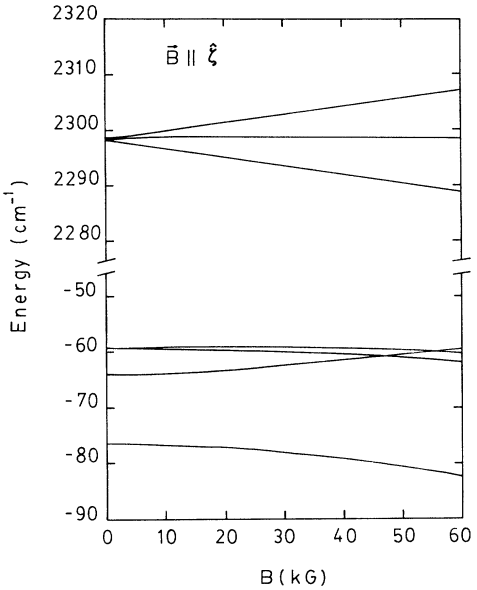

FIG. 1. Magnetic-field dependence of the lowest three energy levels (Γ_1, Γ_2, and Γ_3) originating from the $^5\Gamma_3(T_d)$ multiplet of the tetrahedral crystal potential split further by the trigonal distortion, and of the lowest two levels (Γ_3 and Γ_1) originating from the $^5\Gamma_5(T_d)$ multiplet. The applied magnetic field is parallel to the trigonal axis $\hat{\xi}$. The other levels have also been obtained but, for the sake of clarity, are not displayed in the figure. The parameters used in the calculation are $\lambda = -94.0$ cm^{-1}, $\Delta = 2550.6$ cm^{-1}, $b = 28.0$ cm^{-1}, and $c = -22.0$ cm^{-1}.

Fe^{2+} in CdSe to illustrate the method. We base the fit of the parameters on the optical-absorption lines reported in the near-infrared region of the electromagnetic spectrum by Udo *et al.*,[3] since the precision of the Fourier-transform absorption measurements is greater than that of Raman-scattering data. Subsequently, as a check of

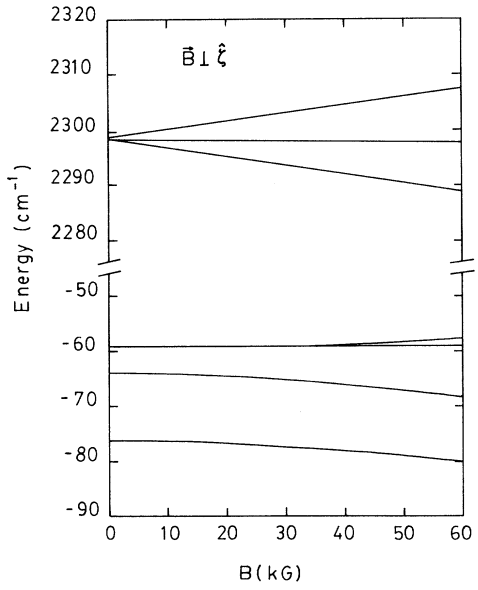

FIG. 2. Same as in Fig. 1 but with an applied magnetic field **B** at right angles to the trigonal axis.

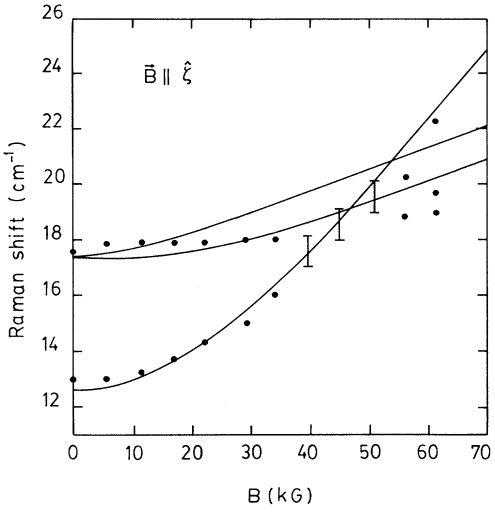

FIG. 3. Raman lines as functions of the magnetic field **B** parallel to $\hat{\xi}$, the trigonal axis. The solid lines are calculated using the parameters listed in the caption to Fig. 1. The experimental points shown are those of Ref. 4. Note that the theoretical curves were obtained using the near-infrared data of Ref. 3 only. We observe that the crossing occurs because the lower line, corresponding to the transition $\Gamma_1 \rightarrow \Gamma_2$ of C_{3v}, belongs to $\Gamma_1 \rightarrow \Gamma_1$ of C_3, the symmetry group when a magnetic field ($\mathbf{B} \| \hat{\xi}$) is present. The other lines correspond to transitions $\Gamma_1 \rightarrow \Gamma_2 + \Gamma_3$ of C_3. Thus they cross rather than interact with one another. The $\Gamma_2(C_3)$ and $\Gamma_3(C_3)$ cross for $B = 120$ kG (not shown in the figure). We have made an exact diagonalization of the 25×25 matrix using the parameters of Ref. 4. Our results (which we do not display) differ somewhat from theirs. In particular the crossing of $\Gamma_2(C_3)$ and of $\Gamma_3(C_3)$ referred to above occurs at $B = 88$ kG instead of near $B = 70$ kG, as it appears to be in Fig. 3(a) of Ref. 4.

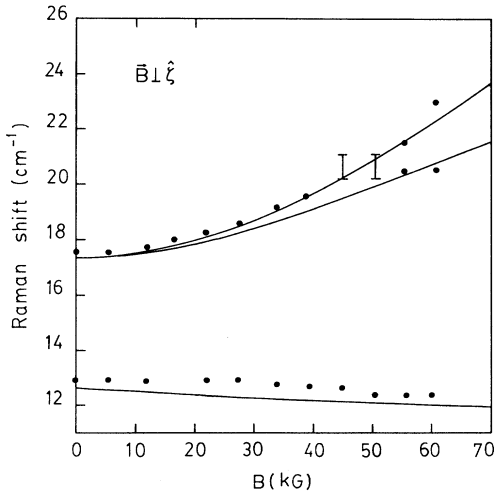

FIG. 4. Same as Fig. 3 but with a magnetic field at right angles to the trigonal axis. For B in the range shown these lines are independent of the particular direction of **B** in the plane perpendicular to $\hat{\xi}$. However, at higher magnetic fields additional anisotropy is expected (see, e.g., Ref. 9) when higher-order contributions to the magnetization become significant.

TABLE III. Matrix $M_{\beta\beta}$ of the Hamiltonian in the states β_i $(i=1,\ldots,4)$.

$M_{\beta\beta}$	β_1	β_2	β_3	β_4
β_1	0	$-\sqrt{2}(\kappa+\lambda)$	0	-2λ
β_2	$-\sqrt{2}(\kappa+\lambda)$	$\Delta_1+\lambda$	2λ	0
β_3	0	2λ	0	$\sqrt{2}(-\kappa+2\lambda)$
β_4	-2λ	0	$\sqrt{2}(-\kappa+2\lambda)$	$\Delta_1-2\lambda$

our values of λ, Δ, b, and c, we calculate the magnetic-field dependence of the two Raman lines observed by Mauger *et al.*[4] and compare our results to the experiment.

The optical-absorption spectrum of CdSe: Fe^{2+} in Ref. 3 was obtained with incident light polarized either in the direction of or at right angles to the trigonal axis. Three lines are observed at energies $E_{\rm I}=2375.4$, $E_{\rm IIa}=2362.8$, and $E_{\rm IIb}=2358.0$ $\rm cm^{-1}$, which are attributed to transitions between the electronic levels of isolated Fe^{2+} ions. They are interpreted as transitions between the three lowest states of Fe^{2+} and the lowest Γ_5 state originating from the excited ${}^5\Gamma_5$ orbital multiplet and splitting into Γ_1 and Γ_3 of C_{3v} in the presence of the trigonal distortion.

The line at $E_{\rm I}=2375.4$ $\rm cm^{-1}$, which is a $\Gamma_1\rightarrow\Gamma_1$ transition for light polarized parallel to $\hat{\xi}$, occurs at the same energy as the $\Gamma_1\rightarrow\Gamma_3$ transition allowed with polarization perpendicular to $\hat{\xi}$. From this we conclude that the lowest Γ_1 and Γ_3 levels of the ${}^5\Gamma_5(T_d)$ multiplet are not split significantly by the trigonal potential. This implies (using the energies in Table VIII of Ref. 2 and within the approximations made there) that

$$c=-\tfrac{9}{4}b\ . \tag{25}$$

Furthermore, in second-order perturbation theory, the energy difference between $E_{\rm IIa}$ and $E_{\rm IIb}$ is simply

$$6\kappa\sigma=E_{\rm IIa}-E_{\rm IIb}=4.8\ \rm cm^{-1}\ , \tag{26}$$

or using Eq. (25), we get

$$\tfrac{7}{2}\sigma b=1.6\ \rm cm^{-1}\ . \tag{27}$$

It should be noted that $E_{\rm IIa}-E_{\rm IIb}=4.8$ $\rm cm^{-1}$ is in agreement with the results of magnetic-susceptibility measurements by Mahoney *et al.*[15] and of Raman scattering by Mauger *et al.*,[4] which yield 4.6 $\rm cm^{-1}$ for the energy difference between Γ_2 and Γ_3. In addition, the order of the levels, namely that Γ_3 lies higher than Γ_2, is consistent with magnetic-susceptibility studies[15] and leads to the condition $b>c/3$. Equations (25) and (27) will give b and c once σ is known. We use $E_{\rm I}$ and $E_{\rm IIa}$ to determine σ and Δ. We have

$$E_{\rm I}=f(\sigma)\Delta+\kappa \tag{28}$$

and

$$E_{\rm IIa}=g(\sigma)\Delta+\kappa(1+4\sigma)\ , \tag{29}$$

where

$$f(\sigma)=1-3\sigma+\tfrac{138}{5}\sigma^2-\tfrac{4866}{125}\sigma^3-\tfrac{1\,427\,946}{3125}\sigma^4+\cdots \tag{30}$$

and

$$g(\sigma)=f(\sigma)-6\sigma^2(1-5\sigma-35\sigma^2)\ . \tag{31}$$

Eliminating Δ from Eqs. (28) and (29), we obtain a relation for σ which can be solved by iteration, namely

$$\sigma=[\tfrac{1}{6}f(\sigma)(E_{\rm I}-E_{\rm IIa}+4\kappa\sigma)]^{1/2} \times(1-5\sigma-35\sigma^2)^{-1/2}(E_{\rm I}-\kappa)^{-1/2}\ , \tag{32}$$

where for $E_{\rm I}$ and $E_{\rm IIa}$ we substitute the experimental values. The iteration procedure converges rapidly to $\sigma=0.036\,657$. From Eq. (28), for example, we then get $\Delta=2546.1$ $\rm cm^{-1}$ and $\lambda=-93.3$ $\rm cm^{-1}$, whereas Eqs. (25) and (27) yield $b=12.5$ $\rm cm^{-1}$ and $c=-28.1$ $\rm cm^{-1}$. This gives the orders of magnitude of λ,Δ,b,c as well as the signs of b and c. Note that the value of λ we just obtained is close to the free-ion value, namely -103 $\rm cm^{-1}$. We take these values of the parameters as our starting point for the numerical diagonalization and finally obtain refined values from the numerical fit. The best fit is ob-

TABLE V. Matrix $M_{\alpha\beta}$ of the Hamiltonian between the states $\alpha_i(i=1,\ldots,5)$ and $\beta_j(j=1,\ldots,4)$. Each element has to be multiplied by $i\epsilon_\xi=i\mu_B B_\xi$.

$M_{\alpha\beta}$	β_1	β_2	β_3	β_4
α_1	2	$-\sqrt{2}$	0	0
α_2	$-\sqrt{2}$	3	0	0
α_3	0	0	-4	$-\sqrt{2}$
α_4	0	0	$-\sqrt{2}$	-3
α_5	0	0	0	0

TABLE IV. Matrix $M_{\gamma^{(\pm)}\gamma^{(\pm)}}$ of the Hamiltonian in the states $\gamma_i^{(\pm)}$ $(i=1,\ldots,8)$

$M_{\gamma^{(\pm)}\gamma^{(\pm)}}$	$\gamma_1^{(\pm)}$	$\gamma_2^{(\pm)}$	$\gamma_3^{(\pm)}$	$\gamma_4^{(\pm)}$	$\gamma_5^{(\pm)}$	$\gamma_6^{(\pm)}$	$\gamma_7^{(\pm)}$	$\gamma_8^{(\pm)}$
$\gamma_1^{(\pm)}$	$\mp2\epsilon_\xi$	$\sqrt{2}(-\kappa+\lambda\mp\epsilon_\xi)$	0	0	0	-2λ	0	$\sqrt{6}\lambda$
$\gamma_2^{(\pm)}$	$\sqrt{2}(-\kappa+\lambda\mp\epsilon_\xi)$	$\Delta_1-\lambda\mp\epsilon_\xi$	0	0	0	$-\sqrt{2}\lambda$	$-\sqrt{6}\lambda$	0
$\gamma_3^{(\pm)}$	0	0	$\pm4\epsilon_\xi$	$-\sqrt{2}(\kappa+2\lambda\pm\epsilon_\xi)$	2λ	0	0	0
$\gamma_4^{(\pm)}$	0	0	$-\sqrt{2}(\kappa+2\lambda\pm\epsilon_\xi)$	$\Delta_1+2\lambda\pm5\epsilon_\xi$	$\sqrt{2}\lambda$	0	0	0
$\gamma_5^{(\pm)}$	0	0	2λ	$\sqrt{2}\lambda$	$\Delta_2\pm2\epsilon_\xi$	0	$\sqrt{6}\lambda$	$\sqrt{3}\lambda$
$\gamma_6^{(\pm)}$	-2λ	$-\sqrt{2}\lambda$	0	0	0	$\Delta_2\mp4\epsilon_\xi$	0	0
$\gamma_7^{(\pm)}$	0	$-\sqrt{6}\lambda$	0	0	$\sqrt{6}\lambda$	0	0	$-\sqrt{2}(\kappa\mp\epsilon_\xi)$
$\gamma_8^{(\pm)}$	$\sqrt{6}\lambda$	0	0	0	$\sqrt{3}\lambda$	0	$-\sqrt{2}(\kappa\mp\epsilon_\xi)$	$\Delta_1\mp\epsilon_\xi$

TABLE VI. Matrix $M_{\alpha\gamma^{(\pm)}}$ of the Hamiltonian between the states α_i and $\gamma_k^{(\pm)}(i=1,\ldots,5;k=1,\ldots,8)$. Each element must be multiplied by $\epsilon_\pm=\frac{1}{2}\mu_B B_\pm$.

$M_{\alpha\gamma^{(\pm)}}$	$\gamma_1^{(\pm)}$	$\gamma_2^{(\pm)}$	$\gamma_3^{(\pm)}$	$\gamma_4^{(\pm)}$	$\gamma_5^{(\pm)}$	$\gamma_6^{(\pm)}$	$\gamma_7^{(\pm)}$	$\gamma_8^{(\pm)}$
α_1	0	$-\sqrt{2}$	$2\sqrt{2}$	0	$\sqrt{2}$	0	$2\sqrt{3}$	0
α_2	$\sqrt{2}$	0	0	$2\sqrt{2}$	1	0	0	$2\sqrt{3}$
α_3	$-2\sqrt{2}$	0	0	$-\sqrt{2}$	0	$\sqrt{2}$	0	0
α_4	0	$-2\sqrt{2}$	$\sqrt{2}$	0	0	1	0	0
α_5	0	0	0	0	$2\sqrt{6}$	0	2	$\sqrt{2}$

tained with $\lambda=-94.0$ cm^{-1}, $\Delta=2550.6$ cm^{-1}, $b=28.0$ cm^{-1}, and $c=-22.0$ cm^{-1}, in close agreement with the result of perturbation theory. With these parameters the lowest Γ_3 and Γ_1 levels originating from the $^5\Gamma_5(T_d)$ manifold are separated by 0.55 cm^{-1}. Table I shows a comparison between theory and experiment for the energies of lines I, IIa, and IIb. The second column shows the results of perturbation theory whereas the third displays the numerical values of $E_{\rm I}$, $E_{\rm IIa}$, $E_{\rm IIb}$ with the appropriate parameters. For comparison we also show the results obtained using the parameters given by Mauger *et al.*[4] We see that the latter are not able to account for the optical-absorption data. Figures 1 and 2 show the magnetic-field dependence of the energy levels of Fe^{2+} involved in the transitions discussed above for two orientations of the magnetic field with respect to the trigonal axis. With the parameters $\lambda=-94.0$ cm^{-1}, $\Delta=2550.6$ cm^{-1}, $b=28.0$ cm^{-1}, and $c=-22.0$ cm^{-1} we also calculate the behavior of the two Raman lines observed by Mauger *et al.*[4] as a function of magnetic field. The results are shown in Figs. 3 and 4 together with the experimental points of Ref. 4. The reasonable agreement between theory and experiment provides a further check of our values of λ, Δ, b, and c.

ACKNOWLEDGMENTS

The authors wish to thank Professor A. K. Ramdas and Dr. M. K. Udo for many useful discussions. Two of us (M.V. and S.R.) are grateful to Professor F. Bassani and his colleagues for their kind hospitality at Scuola Normale Superiore, Pisa when this work was initiated. This work was supported in part by the U.S. National Science Foundation Grant No. DMR-89-13706, by the North Atlantic Treaty Organization, and by Fonds de la Recherche Fondamentale et Collective (Belgium) (Grant No. 2.4515.90).

APPENDIX A

We give the wave functions of the 25 lowest states of Fe^{2+} as a combination of the orbital states u_i,v_j $(i=1,-1;j=1,0,-1)$ defined in Eqs. (7) and the spin states χ_μ $(\mu=2,1,0,-1,-2)$. They are obtained using the Clebsch-Gordan coefficients appropriate for C_{3v} symmetry and can be classified as follows:

$$\alpha_1=2^{-1/2}(u_1\chi_{-1}+u_{-1}\chi_1)\,,$$
$$\alpha_2=2^{-1/2}(v_1\chi_{-1}+v_{-1}\chi_1)\,,$$
$$\alpha_3=2^{-1/2}(-u_1\chi_2+u_{-1}\chi_{-2})\,,$$
$$\alpha_4=2^{-1/2}(-v_1\chi_2+v_{-1}\chi_{-2})\,,$$
$$\alpha_5=v_0\chi_0\,,$$

which belong to Γ_1 of C_{3v};

$$\beta_1=-2^{-1/2}i(u_1\chi_{-1}-u_{-1}\chi_1)\,,$$
$$\beta_2=-2^{-1/2}i(v_1\chi_{-1}-v_{-1}\chi_1)\,,$$
$$\beta_3=2^{-1/2}i(u_1\chi_2+u_{-1}\chi_{-2})\,,$$
$$\beta_4=2^{-1/2}i(v_1\chi_2+v_{-1}\chi_{-2})\,,$$

belonging to Γ_2 of C_{3v}; and

$$\gamma_1^{(\pm)}=\mp u_{\mp1}\chi_{\mp1}\,,$$
$$\gamma_2^{(\pm)}=\mp v_{\mp1}\chi_{\mp1}\,,$$
$$\gamma_3^{(\pm)}=u_{\mp1}\chi_{\pm2}\,,$$
$$\gamma_4^{(\pm)}=v_{\mp1}\chi_{\pm2}\,,$$
$$\gamma_5^{(\pm)}=v_0\chi_{\pm1}\,,$$
$$\gamma_6^{(\pm)}=\pm v_0\chi_{\mp2}\,,$$
$$\gamma_7^{(\pm)}=u_{\pm1}\chi_0\,,$$
$$\gamma_8^{(\pm)}=v_{\pm1}\chi_0\,.$$

TABLE VII. Matrix $M_{\beta\gamma^{(\pm)}}$ of the Hamiltonian between the states β_j and $\gamma_k^{(\pm)}(j=1,\ldots,4;k=1,\ldots,8)$. Each element is to be multiplied by $\mp i\epsilon_\pm$.

$M_{\beta\gamma^{(\pm)}}$	$\gamma_1^{(\pm)}$	$\gamma_2^{(\pm)}$	$\gamma_3^{(\pm)}$	$\gamma_4^{(\pm)}$	$\gamma_5^{(\pm)}$	$\gamma_6^{(\pm)}$	$\gamma_7^{(\pm)}$	$\gamma_8^{(\pm)}$
β_1	0	$\sqrt{2}$	$2\sqrt{2}$	0	$\sqrt{2}$	0	$-2\sqrt{3}$	0
β_2	$-\sqrt{2}$	0	0	$2\sqrt{2}$	1	0	0	$-2\sqrt{3}$
β_3	$-2\sqrt{2}$	0	0	$\sqrt{2}$	0	$\sqrt{2}$	0	0
β_4	0	$-2\sqrt{2}$	$-\sqrt{2}$	0	0	1	0	0

TABLE VIII. Matrix $M_{\gamma^{(+)}\gamma^{(-)}}$ of the Hamiltonian between the states $\gamma_k^{(+)}$ and $\gamma_k^{(-)}(k=1,\ldots,8)$. Each element is to be multiplied by ϵ_+.

$M_{\gamma^{(+)}\gamma^{(-)}}$	$\gamma_1^{(-)}$	$\gamma_2^{(-)}$	$\gamma_3^{(-)}$	$\gamma_4^{(-)}$	$\gamma_5^{(-)}$	$\gamma_6^{(-)}$	$\gamma_7^{(-)}$	$\gamma_8^{(-)}$
$\gamma_1^{(+)}$	0	0	0	0	-2	0	$-2\sqrt{6}$	0
$\gamma_2^{(+)}$	0	0	0	0	$-\sqrt{2}$	0	0	$-2\sqrt{6}$
$\gamma_3^{(+)}$	0	0	0	0	0	-2	0	0
$\gamma_4^{(+)}$	0	0	0	0	0	$-\sqrt{2}$	0	0
$\gamma_5^{(+)}$	2	$\sqrt{2}$	0	0	0	-4	0	0
$\gamma_6^{(+)}$	0	0	2	$\sqrt{2}$	4	0	0	0
$\gamma_7^{(+)}$	$2\sqrt{6}$	0	0	0	0	0	0	2
$\gamma_8^{(+)}$	0	$2\sqrt{6}$	0	0	0	0	-2	0

$\gamma_i^{(\pm)}$ belongs to the first (second) row of Γ_3 of C_{3v}, i.e., they behave as $-(\xi+i\eta)$ and $(\xi-i\eta)$, respectively, under the operations of the group.

APPENDIX B

The submatrices $M_{\mu\nu}$ $(\mu,\nu=\alpha,\beta,\gamma^{(+)},\gamma^{(-)})$ of the Hamiltonian in the states α_i, β_j, and $\gamma_k^{\pm}$ $(i=1,\ldots,5;j=1,\ldots,4;k=1,\ldots,8)$ of Appendix A are given in Tables II–VIII in terms of the parameters $\lambda,\kappa=b-c/3$, $\Delta_1=\Delta+\kappa$, $\Delta_2=\Delta+\kappa-3b-(4c/3)$, $\epsilon_\xi=\mu_B B_\xi$, and $\epsilon_\pm=\mu_B B_\pm/2=\mu_B(B_\xi\pm iB_\eta)/2$. In Tables II, III, and IV the constant term $-(18a/5)+(7c/15)$ has been removed from all diagonal matrix elements.

APPENDIX C

We give the coefficients ρ_1 and ρ_2 intervening in Eq. (24) in terms of the energies p_5, p_6, p_8, and p_9 of Eqs. (18) and (19). They are

$$\rho_1=\frac{3+p_{5,8}^2-4p_{5,8}+2p_{5,8}p_{6,9}}{p_{5,8}(p_{5,8}-p_{6,9})}$$

and

$$\rho_2=\frac{(p_{6,9}-2p_{5,8})\rho_1^2+(p_{5,8}+p_{6,9}-4)\rho_1-30-41p_{5,8}-2p_{6,9}+18p_{5,8}^2-44p_{6,9}^2-92p_{5,8}p_{6,9}}{p_{5,8}(p_{5,8}-p_{6,9})}\,.$$

[1]See, for example, *Diluted Magnetic Semiconductors,* Semiconductors and Semimetals Vol. 25, edited by J. K. Furdyna and J. Kossut (Academic, Boston, 1988).

[2]M. Villeret, S. Rodriguez, and E. Kartheuser, J. Appl. Phys. **67**, 4221 (1990).

[3]M. K. Udo, M. Villeret, I. Miotkowski, A. J. Mayur, A. K. Ramdas, and S. Rodriguez, Phys. Rev. B **46**, 7459 (1992).

[4]A. Mauger, D. Scalbert, J. A. Gaj, J. Cernogora, and C. Benoit à la Guillaume, Phys. Rev. B **43**, 7102 (1991).

[5]Note that Mauger *et al.* (Ref. 4) use a different set of axes, namely $\hat{\xi}\|[2\bar{1}\,\bar{1}]$, $\hat{\eta}\|[01\bar{1}]$, and $\hat{\zeta}\|[111]$. This gives rise to a change in sign in the second term of Eq. (3). This is most easily understood if one writes Eqs. (3) and (4) in terms of spherical harmonics. We have

$$V_c(T_d)=(-8a'\pi^{1/2}/45)\langle r^4\rangle \times\sum_i\{\,Y_4^0(\theta_i,\phi_i) -(10/7)^{1/2}[\,Y_4^3(\theta_i,\phi_i)-Y_4^{-3}(\theta_i,\phi_i)]\}$$

and

$$V_c(C_{3v})=(-4b'/3)(\pi/5)^{1/2}\langle r^2\rangle\sum_i Y_2^0(\theta_i,\phi_i) +(4c'\pi^{1/2}/45)\langle r^4\rangle\sum_i Y_4^0(\theta_i,\phi_i)\,,$$

where the angle ϕ is referred to $[11\bar{2}]$. In Ref. 4 the azimuth ϕ is referred to $[2\bar{1}\,\bar{1}]$ and is shifted with respect to that in the present work by $-\pi/3$, which changes the sign of Y_4^3 and Y_4^{-3}.

[6]M. Villeret, S. Rodriguez, and E. Kartheuser, Physica B **162**, 89 (1990). Note that in Table VIII of this reference there are the following obvious misprints: the last term in ϵ_2'' should read $-5^{1/2}|v_-,1\rangle$ and the wave functions $\delta_1'',\delta_2'',\delta_3''$ belong to Γ_4.

[7]M. Villeret, S. Rodriguez, and E. Kartheuser, Phys. Rev. B **41**, 10 028 (1990); **42**, 11 375(E) (1990), where a trivial numerical error in Fig. 2 of this reference is corrected. See also Refs. 8 and 9.

[8]M. Villeret, S. Rodriguez, and E. Kartheuser, Solid State Commun. **75**, 21 (1990).

[9]M. Villeret, S. Rodriguez, and E. Kartheuser, Phys. Rev. B **43**, 3443 (1991).

[10]K. W. H. Stevens, Proc. Phys. Soc. London **65**, 209 (1952).

[11]Using a method described by A. Abragam and B. Bleaney [*Electron Paramagnetic Resonance of Transition Ions* (Clarendon, Oxford, 1970)], it is possible to relate a, b, and c to the parameters A_4^0, B_2^0, and B_4^0 used in Ref. 4. The relations are

$$a=(\tfrac{5}{28})\pi^{-1/2}\langle r^4\rangle A_4^0\,,$$

$$b=-\tfrac{1}{14}(5/\pi)^{1/2}\langle r^2\rangle B_2^0\,,$$

$$c=-(\tfrac{5}{14})\pi^{-1/2}\langle r^4\rangle B_4^0\,.$$

[12]We describe the irreducible representations according to the nomenclature in G. F. Koster, J. O. Dimmock, R. G. Wheeler, and H. Statz, *Properties of the Thirty-Two Point Groups* (MIT, Cambridge, MA, 1966).

[13]Using Ref. 11, we can express the matrix elements in Eqs. (8) in terms of the constants A_4^0, B_2^0, and B_4^0 used by Mauger *et al.* (Ref. 4), i.e.,

$$\langle u_1|V_c|u_1\rangle=\langle u_{-1}|V_c|u_{-1}\rangle=-\frac{3}{2\sqrt{\pi}}\langle r^4\rangle(\tfrac{3}{7}A_4^0+\tfrac{1}{9}B_4^0)\ .$$

$$\langle v_0|V_c|v_0\rangle=\frac{1}{7\sqrt{\pi}}(3\langle r^4\rangle A_4^0+\sqrt{5}\langle r^2\rangle B_2^0+3\langle r^4\rangle B_4^0)\ ,$$

$$\langle v_1|V_c|v_1\rangle=\langle v_{-1}|V_c|v_{-1}\rangle$$

$$=\frac{1}{7\sqrt{\pi}}(3\langle r^4\rangle A_4^0-\tfrac{1}{2}\sqrt{5}\langle r^2\rangle B_2^0-\tfrac{1}{3}\langle r^4\rangle B_4^0)\ .$$

The nonvanishing off-diagonal matrix elements are all equal to

$$\langle u_1|V_c|v_1\rangle=-\frac{1}{7\sqrt{2\pi}}(-\sqrt{5}\langle r^2\rangle B_2^0+\tfrac{5}{3}\langle r^4\rangle B_4^0)\ .$$

It is interesting to note that these matrix elements are identical to those of Eqs. (11) of Ref. 4 but they have been calculated *not* with the wave functions given in Eqs. (8) of Ref. 4 but with the wave functions in Table VI of Ref. 2 with $\alpha=\arccos(3^{-1/2})$. The difference in sign between $\langle u_1|V_c|v_1\rangle$ and Eq. (14) of Ref. 4 is due to the choice of $\hat{\xi}$ axis to measure the azimuthal angle. We also remark that the symmetry assignments in Fig. 1 of Ref. 4 and in their text are incorrect (see, e.g., Ref. 2 for the correct assignments).

[14]G. A. Slack, S. Roberts, and J. T. Vallin, Phys. Rev. **187**, 511 (1969).

[15]J. P. Mahoney, C. C. Lin, W. H. Brumage, and F. Dorman, J. Chem. Phys. **53**, 4286 (1970).